Eur. Phys. J. D **9**, 141–144 (1999)

THE EUROPEAN
PHYSICAL JOURNAL D
EDP Sciences

Mass spectrometric characterization of iron clusters produced by laser pyrolysis and photolysis of $Fe(CO)_5$ in a flow reactor

F. Huisken[1], B. Kohn[1], R. Alexandrescu[2], and I. Morjan[2]

[1] Max-Planck-Institut für Strömungsforschung, Bunsenstrasse 10, D-37073 Göttingen, Germany
[2] National Institute for Lasers, Plasma and Radiation Physics, P.O. Box MG-36, R-76900 Bucharest, Romania

Received: 31 August 1998 / Received in final form: 21 October 1998

Abstract. Laser-induced decomposition of iron pentacarbonyl in a flow reactor has been used to produce iron clusters and nanoparticles. The as-synthesized species are extracted from the reaction zone by a conical nozzle and expanded into the source chamber of a cluster beam apparatus where, after having traversed a differential chamber, they are analyzed *in situ* with a time-of-flight mass spectrometer. Three different lasers have been employed to accomplish decarbonylation of the $Fe(CO)_5$ molecules. A pulsed CO_2 laser ($\lambda = 10.6\,\mu$m) was used to excite a mixture of SF_6 and $Fe(CO)_5$ and to *pyrolyze* the iron pentacarbonyl. Laser *photolysis* was performed by directly dissociating the $Fe(CO)_5$ molecules with UV radiation. For this purpose, we used the tripled ($\lambda = 355$ nm) and quadrupled ($\lambda = 266$ nm) Nd:YAG laser as well as an ArF excimer laser ($\lambda = 193$ nm). The mass spectrometric analysis showed that only the Nd:YAG laser produced high purity iron clusters which were essentially free of contamination.

PACS. 61.46.+w Clusters and nanoparticles – 81.15.Gh Chemical vapor deposition – 82.50.Fv Photolysis – 82.80.Ms Mass spectrometry

1 Introduction

Among the various transition metal clusters, one of the most extensively studied systems is probably the iron cluster system. This is due to the high catalytic activity of iron and its oxides in many chemical processes such as hydrogenation and the synthesis of ammonia and hydrocarbons [1]. Clusters and nanoparticles, containing up to a few thousand metal atoms, possess a high ratio of surface to bulk atoms, and therefore, they may dramatically increase the efficiency of a catalytic process, compared to more bulk-like catalyzers. As a result, several studies have been carried out to investigate the chemical behavior of iron clusters [2–8]. Whereas some reactions (*e.g.* H_2 chemisorption) revealed a pronounced size dependence [2, 7] others were quite monotonic, such as the chemisorption of CO [3].

Up to date, much work has been done with iron clusters containing up to $n = 25$ atoms. Typically they were produced by laser vaporization of bulk iron. Considerably larger iron clusters, *i.e.* nanoscaled clusters or "nanoclusters" with diameters up to $d = 100$ nm were synthesized from gas phase reactants. The most widely used precursor was iron pentacarbonyl which was decomposed chemically [9] or by CO_2-laser-induced pyrolysis [10–13]. With this technique, γ-Fe particles with fcc structure and diameters around 13 nm [11] or iron-oxide-based nanoparticles with an average size of 30 nm [13] were obtained. Using the same method, Eklund and coworkers [10] reported the production of nanosized α-Fe and iron carbides. Among other possible precursors, iron pentacarbonyl has two distinct properties making it attractive for conventional and laser CVD processes [14]: (1) sufficiently high vapor pressure and (2) low activation energy for breaking the metal-CO bonds. Thus, it offers a rather easy way for the production of metal atoms and clusters. A slight disadvantage represents the fact that $Fe(CO)_5$ absorbs only very weakly in the emission range of the CO_2 laser, so that the admixture of a strong absorber gas, such as SF_6, is required [11–13]. Ideally, the sensitizer will transfer the absorbed energy to the metal carbonyl by collisions, without being involved in the reaction sequence.

Most experimental studies devoted to small Fe_n clusters ($n < 25$) were carried out in molecular beams using a laser vaporization source to produce the iron clusters. On the other hand, laser-driven CVD reactors yield particle sizes with $d > 10$ nm which may be too large for many applications. To close the gap between small clusters ($n < 25$) and large nanoparticles with diameters larger than 10 nm and to study the intermediate sizes, we have recently developed a novel cluster source, which combines the laser-driven flow reactor with a supersonic expansion of the nascent clusters into a high-vacuum molecular beam apparatus [15]. While the first experiments were devoted to carbon clusters and fullerenes using C_2H_2 as precursor gas [16, 17], the later studies focused on the production and characterization of silicon clusters [17, 18]. It was shown that the source is indeed capable of producing silicon nanoclusters in the desired size regime, with diameters between 1 and 10 nm [18, 19].

With the same setup, we have recently produced iron clusters and nanoparticles by laser-induced decomposition of $Fe(CO)_5$ using three different lasers: a CO_2 laser, a Nd:YAG laser, and an excimer laser. The effect of the different laser frequencies on the composition and purity of the clusters has been studied with a time-of-flight mass spectrometer. Using its high resolution mode, we were able to resolve the isotopic composition of medium-sized iron clusters.

2 Experimental

The experiments have been carried out in a cluster beam apparatus which has been described in detail earlier [15–18]. It consists of three stages, the source chamber enhousing the flow reactor, a pressure-reducing differential chamber, and the ultra-high-vacuum chamber containing the time-of-flight mass spectrometer (TOFMS). The latter can be operated as ordinary Wiley-McLaren-type TOFMS or as linear reflectron-type mass spectrometer [18]. Ionization of the clusters is achieved by the nonfocused radiation of an ArF excimer laser ($\lambda = 193$ nm) with typically 3 mJ/pulse.

The iron clusters were produced in the CVD reactor by exciting the confined gas flow of iron pentacarbonyl with the radiation of various pulsed laser sources. Since the $Fe(CO)_5$ molecule does not absorb in the 10 μm region, SF_6 was used as sensitizer when the CO_2 laser was employed. For this purpose, the SF_6 gas was bubbled with a flow rate of 6 sccm through the stainless steel reservoir containing a sample of liquid $Fe(CO)_5$. The reservoir was kept at a temperature of 20 °C which resulted in a $Fe(CO)_5$ vapor pressure of 29 mbar. In order to confine the sensitized gas mixture to the flow axis, He was flushed with a flow rate of 1100 sccm through the outer tube of the CVD reactor. The total pressure was maintained at 260 mbar.

During the course of the experiment, we replaced the CO_2 laser by either a Nd:YAG laser (3rd and 4th harmonics) or an ArF excimer laser. In contrast to the IR radiation of the CO_2 laser which causes a *pyrolysis* of the thermally activated $Fe(CO)_5$ molecules, the absorption of the UV photons at 355, 266, and 193 nm results in the prompt dissociation of $Fe(CO)_5$ via electronic excitation (*photolysis*). A major advantage of using the UV lasers is that SF_6 is not needed anymore. The laser energies applied to photolyze the iron pentacarbonyl were 15, 19, and 20 mJ/pulse, for 355, 266, and 193 nm, respectively. The iron clusters produced by condensation of the refractory portion of the dissociation products were extracted from the reaction zone by a conical nozzle of 0.3 mm diameter.

3 Results and discussion

The first experiments were carried using the pulsed CO_2 laser to pyrolize a mixture of $Fe(CO)_5$ and SF_6. The resulting pulsed cluster beam was analyzed with the TOF mass spectrometer at various delays between the CO_2 laser and the ionizing excimer laser. Two different "snap shots" are shown in Fig. 1. As is indicated in the figure, the regular series of larger peaks can be immediately assigned to iron clusters (Fe_n). In contrast, the smaller peaks in-between are due to impurities which cannot be specified at the present level of resolution; but later we will show that fluorine, sulfur, and CO being chemisorbed on Fe_n are responsible for these peaks. The main spectrum of Fig. 1 was recorded with a delay of $\tau = 370\,\mu$s and reflects the situation in the earlier part of the cluster pulse, while the inset spectrum shows the corresponding distribution at a later time ($\tau = 450\,\mu$s). It appears that the smaller clusters have a larger velocity and therefore reach the ionization region somewhat earlier than the heavier (and slower) clusters. If we adjust the delay to values larger than 500 μs we even observe iron clusters with diameters around 4 nm. In our detailed study on silicon clusters [18, 19], we have shown that this size-dependent velocity can be exploited to achieve a substantial narrowing of the cluster size distribution (*quasi* size selection) by interrupting the pulsed cluster beam with a slotted disk chopper operated at fixed phase with respect to the CO_2 laser. It is clear that the same technique can also be applied here.

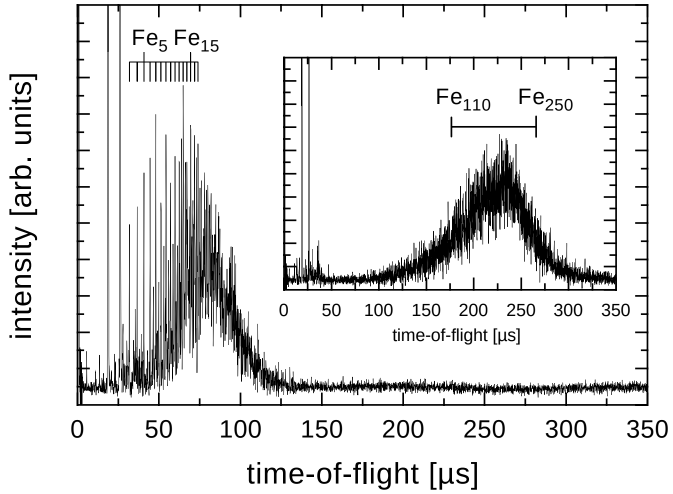

Fig. 1. Mass spectra of iron clusters produced by CO_2-laser-induced pyrolysis of $Fe(CO)_5$. The spectra have been measured at two different delays between CO_2 laser and ionizing laser: 370 μs (main spectrum) and 450 μs (inset).

The approximate intensity of the Fe cluster beam produced with the CO_2 laser was determined with a microbalance positioned 230 mm downstream from the nozzle exit. The deposition rate of 7 ng/min on a surface of 6 mm diameter can be translated into a molecular beam intensity of $\sim 5 \times 10^{18}$ Fe atoms per second and steradian (during the pulse).

In the following experiment, we have replaced the CO_2 laser by a Nd:YAG laser whose 1064 nm fundamental was either tripled or quadrupled. As has been noted before, the corresponding photons can be directly absorbed by the $Fe(CO)_5$ molecules so that a sensitizer is not needed. Therefore, instead of SF_6, helium was bubbled through the

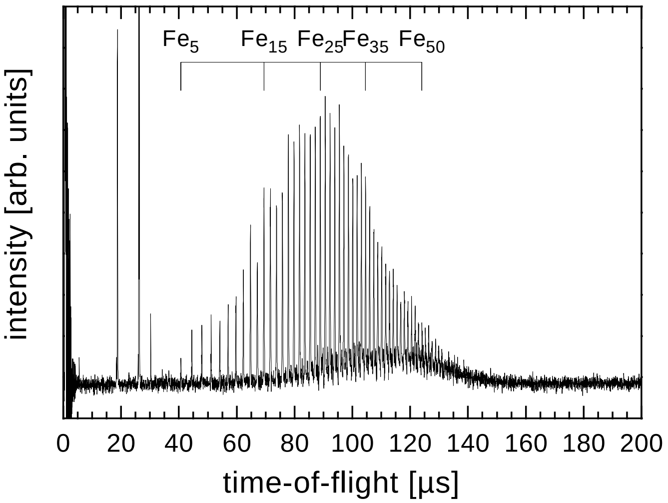

Fig. 2. Mass spectrum of iron clusters produced by photolysis of iron pentacarbonyl with the fourth harmonic (266 nm) of a pulsed Nd:YAG laser.

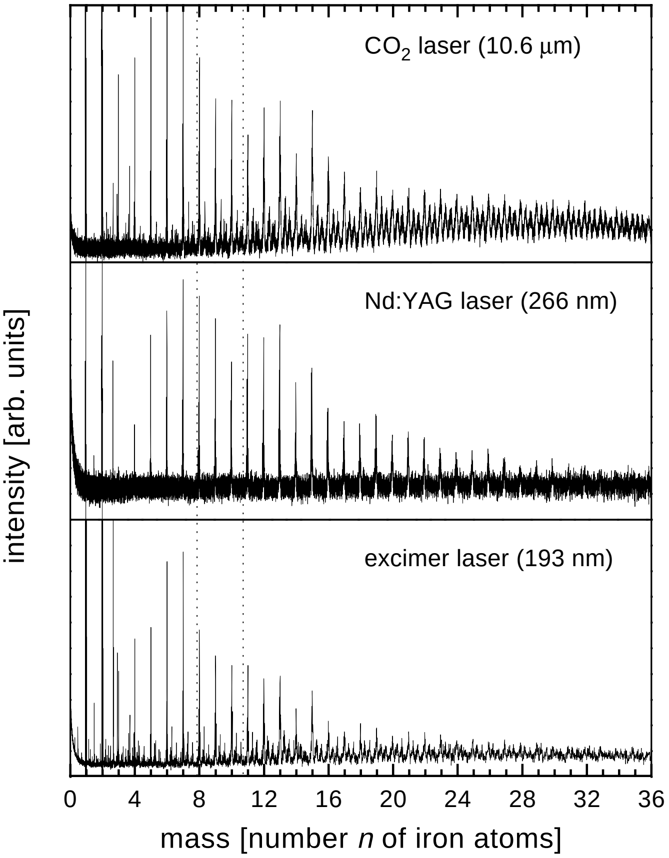

Fig. 3. Comparison of mass spectra measured using different laser sources to decompose the $Fe(CO)_5$. Upper spectrum: CO_2 laser, 10.6 μm, 17 mJ, with SF_6 as sensitizer; middle spectrum: 4th harmonic of Nd:YAG laser, 266 nm, 19 mJ, without SF_6; bottom spectrum: ArF excimer laser, 193 nm, 20 mJ, without SF_6.

iron pentacarbonyl reservoir. A typical spectrum obtained under these conditions with the 4th harmonic (266 nm) of the Nd:YAG laser is shown in Fig. 2. It features a broad iron cluster distribution peaking around Fe_{25}. In contrast to the spectra obtained with the CO_2 laser, the individual iron cluster peaks are now much better resolved and the satellite peaks, encountered in-between, are significantly reduced. Using the 355 nm output of the Nd:YAG laser, we obtained qualitatively the same results; but the intensity of the cluster beam was significantly reduced, due to the smaller absorption cross section at this wavelength [20].

To obtain more detailed information on the kind of impurity atoms or molecules captured by the iron clusters in the reaction zone, the TOFMS was operated with the reflecting field [18] which ensured significantly improved energy resolution. In this high resolution mode, we have carried out a comparative study employing the CO_2 laser, the 4th harmonic of the Nd:YAG laser (as described before), and, in addition, an ArF excimer laser ($\lambda = 193$ nm) to produce the iron clusters. The results of this study are presented in Fig. 3. To facilitate the assignment, the x axis has been calibrated to indicate the number of atoms in the iron clusters. Aside from some background lines below $n = 4$, the more pronounced peaks are clearly assigned to iron clusters. When the $Fe(CO)_5$ is decomposed by the 266 nm radiation of the Nd:YAG laser we observe only the pure iron cluster peaks. However, when we use the CO_2 or excimer laser, at least two satellite peaks appear in-between. It is clearly seen that, compared with the pure Fe_n peaks, they become more pronounced as the cluster size increases.

In order to show the whole information contained in these high-resolution mass spectra, we have blown up the horizontal scale for the mass range indicated by the two vertical dashed lines. These expanded spectra are given in Fig. 4. Now a wealth of structures becomes visible which can be readily assigned as indicated in the figure. At first it must be noted that the pure iron cluster peaks (Fe_8, Fe_9, and Fe_{10}) display a regular fine structure which depends only weakly on the cluster size. This fine structure is due to the natural distribution of isotopes, the iron cluster is made of (5.9% ^{54}Fe, 92.0% ^{56}Fe, and 2.1% ^{57}Fe, considering only the three most abundant isotopes). The intermediate peaks in the upper spectrum can be attributed to $Fe_n{\cdot}F$, $Fe_n{\cdot}CO$, $Fe_n{\cdot}S$, and $Fe_n{\cdot}F_2$ of which the fluorinated iron clusters are the most important ones. They are of course a reminiscence of the SF_6 molecules which were introduced as sensitizer and which were partially dissociated in the laser field. It is interesting to note that the satellite peaks have the same fine structure, being the signature of the iron clusters. The middle spectrum of Fig. 4 clearly shows that the iron clusters are free of impurities if they are produced by $Fe(CO)_5$ photolysis at 266 nm. In contrast, if 193 nm photons are used to dissociate the iron pentacarbonyl another set of satellite peaks is observed. The most important ones are assigned to $Fe_n{\cdot}O$ and $Fe_n{\cdot}O_2$, indicating that the CO groups abstracted from the iron pentacarbonyl are partially dissociated within the same laser pulse. The weaker lines are attributed to $Fe_n{\cdot}C$ and $Fe_n{\cdot}CO$. The dissociation of CO with 193 nm photons proceeds from an excited state above the ground state dissociation energy

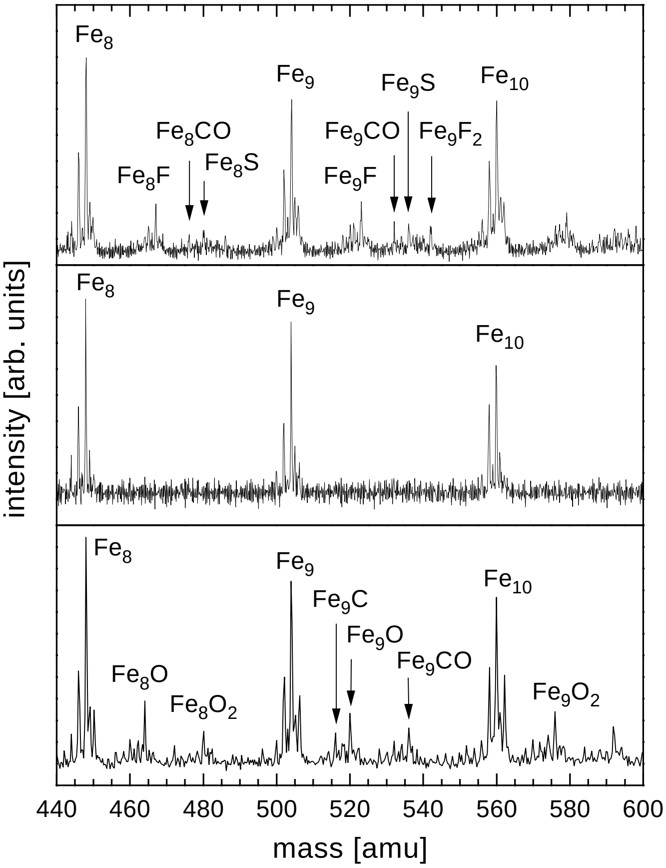

Fig. 4. Expanded view of a portion of the high-resolution mass spectra indicated in Fig. 3 by the dashed lines.

($D_0 = 11.09\,\text{eV}$) which is reached by a resonant 2-photon transition via the $a^3\Pi$ state [21]. Using the 4th harmonic of the Nd:YAG laser, three photons are required with the first step being *non*resonant. This explains why the dissociation of CO is not observed in the Nd:YAG laser experiment.

We have calculated the theoretical natural isotope composition of Fe$_n$ clusters with $n = 8$, 9, and 10 and compared the results with the experimental data. For all lasers used, the agreement was very satisfactory, except for the peaks at mass $m = m(^{56}\text{Fe}_n) + 2$ amu for which the experimental intensities were always larger. This finding can possibly be explained by assuming that H_2 molecules from the residual gas were chemisorbed on the iron clusters.

4 Summary

Using various laser sources in the IR and UV, we have shown that laser-induced decomposition of Fe(CO)$_5$ in a gas flow reactor constitutes an attractive method to produce a molecular beam of iron clusters and nanoparticles. While the CO$_2$-laser-driven operation requires the usage of a sensitizer such as SF$_6$, UV lasers can be directly used to decompose the iron-containing precursor. In the experiment with the CO$_2$ laser, we observed, besides pure iron clusters, also fluorinated iron clusters, indicating that the SF$_6$ molecules were partially decomposed by the intense laser field. In contrast, high purity iron clusters could be produced under conditions where no sensitizer was required, namely with the fourth harmonic of the Nd:YAG laser. The application of higher photon energies, as delivered from an ArF excimer laser, resulted in a partial dissociation of the carbonyl molecules and the following oxidation of the iron clusters to Fe$_n$·O and Fe$_n$·O$_2$.

This work was supported by the Deutsche Forschungsgemeinschaft in the frame of its Schwerpunktprogramm Fine Solid Particles and by a bilateratal cooperation between FRG and Romania (WTZ RUM-008-97).

References

1. I.M. Campbell: *Catalysis at Surfaces* (Chapman and Hall, London, New York 1988)
2. S.C. Richtmeier, E.K. Parks, K. Liu, L.G. Pobo, S.J. Riley: J. Chem. Phys. **82**, 3659 (1985)
3. M.D. Morse, M.E. Geusic, J.R. Heath, R.E. Smalley: J. Chem. Phys. **83**, 2293, (1985)
4. D.M. Cox, K.C. Reichman, D.J. Trevor, A. Kaldor: J. Chem. Phys. **88**, 111 (1988)
5. E.K. Parks, G.C. Nieman, L.G. Pobo, S.J. Riley: J. Chem. Phys. **88**, 6260 (1988)
6. P. Schnabel, M.P. Irion, K.G. Weil: J. Phys. Chem. **95**, 9688 (1991)
7. J. Conceicao, R.T. Laaksonen, L.-S. Wang, T. Guo, P. Nordlander, R.E. Smalley: Phys. Rev. B **51**, 4668 (1995)
8. L.-S. Wang, H.-S. Cheng, J. Fan: J. Chem. Phys. **102**, 9480 (1995)
9. Y. Sawada, Y. Kageyama, M. Iwata, A. Tasaki: Jpn. J. Appl. Phys. **31**, 3858 (1992)
10. X.-X. Bi, B. Granguly, G.P. Huffman, F.E. Huggins, M. Endo, P.C. Ecklund: J. Mater. Res. **8**, 1666 (1993)
11. T. Majima, R. Miyahara, K. Haneda, M. Takami: Jpn. J. Appl. Phys. **33**, L223 (1994)
12. X.Q. Zhao, F. Zheng, Y. Liang, Z.Q. Hu, Y.B. Xu: Mater. Lett. **21**, 285 (1994)
13. R. Alexandrescu, I. Morjan, A. Crunteanu, S. Cojocaru, S. Petcu, V. Teodorescu, F. Huisken, B. Kohn, M. Ehbrecht: Mater. Chem. Phys. **55**, 115 (1998)
14. R. Alexandrescu: Appl. Surf. Sci. **106**, 28 (1996)
15. M. Ehbrecht, H. Ferkel, V.V. Smirnov, O.M. Stelmakh, W. Zhang, F. Huisken: Rev. Sci. Instrum. **66**, 3833 (1995)
16. M. Ehbrecht, M. Faerber, F. Rohmund, V.V. Smirnov, O.M. Stelmakh, F. Huisken: Chem. Phys. Lett. **214**, 34 (1993)
17. M. Ehbrecht, H. Ferkel, V.V. Smirnov, O.M. Stelmakh, W. Zhang, F. Huisken: Surf. Rev. Lett. **3**, 807 (1996)
18. M. Ehbrecht, F. Huisken: Phys. Rev. B **59**, 2975 (1999)
19. M. Ehbrecht, B. Kohn, F. Huisken, M.A. Laguna, V. Paillard: Phys. Rev. B **56**, 6958 (1997)
20. J.T. Yardley, B. Gitlin, G. Nathanson, A.M. Rosan: J. Chem. Phys. **74**, 370 (1981)
21. J. Bokor, J. Zavelovich, C.K. Rhodes: J. Chem. Phys. **72**, 965 (1980)